

Simulation for separation of hydrogen and carbon monoxide by adsorption on single-walled carbon nanotubes

Chong Gu^a, Guang-Hua Gao^{a,*}, Yang-Xin Yu^a, Tomoshige Nitta^b

^a Department of Chemical Engineering, Tsinghua University, Beijing 100084, China

^b Division of Chemical Engineering, Graduate School of Engineering Science, Osaka University, Toyonaka, Osaka 560, Japan

Received 10 March 2001; accepted 23 July 2001

Abstract

In this paper, the separation of binary gas mixture carbon monoxide and hydrogen using single-walled carbon nanotubes (SWNTs) is studied by grand canonical Monte Carlo (GCMC) simulation. All of the particle–particle interactions between hydrogen, carbon monoxide and carbon are modeled with Lennard–Jones potential. Widom test particle method in NVT ensemble is used in determining chemical potentials of the two components of the fluid. It can be concluded from the adsorption isotherms at 293.15 K that the selectivity of carbon monoxide decreases with the increase of the bulk pressure. In the adsorption isostatics at 0.157 MPa, the selectivity has a maximum along with the increase of temperature. However, to given pressure and temperature, the selectivity fluctuates violently with different van der Waals (VDW) distances or diameters of carbon nanotubes. For example, at 0.157 MPa, 293.15 K, diameter of 0.892 nm and VDW distance of 1 nm, with the feed containing hydrogen and carbon monoxide both 50 mol%, carbon monoxide could be enriched up to 98 mol% in the adsorbate, so that the selectivity comes to 60. It can be indicated that carbon nanotube, as a novel material developed in the past 10 years, can make a very effective separation tool of certain gas mixtures. © 2002 Elsevier Science B.V. All rights reserved.

Keywords: Carbon nanotubes; Adsorption; Separation; Monte Carlo simulation

1. Introduction

Adsorptive separation of particular gaseous mixtures is a viable industrial process, where one component must be selectively adsorbed on a suitable adsorbent relative to the other. However, the properties of gas mixtures adsorbed in small spaces are quite different from those in bulk phases. Since microporous membranes and adsorbates are routinely used in industrial separation processes, understanding these effects is vital for developing new separation technologies and optimizing currently used techniques. Selectivity in microporous adsorbates is controlled by a number of factors: the adsorbate–adsorbate

* Corresponding author. Tel.: +86-10-62782558; fax: +86-10-62770304.
E-mail address: gaogh@mail.tsinghua.edu.cn (G.-H. Gao).

interactions for like and unlike molecules including the strength of adsorbate–adsorbent interactions, as well as geometric considerations such as micropore width and the size and shape of the adsorptive species.

Most of the studies on adsorptive separation are based on carbon sorbents. Several research groups have carried out experimental studies in this area. Park et al. [1] introduced a new kind of sorbent structure, which arranges activated carbon and zeolite in layers alternatively. Using different selectivities of the two sorbents toward gas mixture, hydrogen gas with relatively high purity can be obtained. Rege et al. [2] combine 13X-zeolite, γ - Al_2O_3 , natural-zeolite, K^+ -zeolite and Ca^{2+} -zeolite together to make pre-purification of nitrogen and oxygen in air. Clarkson [3] studied the effects of different moisture content on the selectivity of carbon sorbents. As discovered by Iijima [4] in 1991, carbon nanotubes can be obtained by rolling up a single layer or multiple layers of graphite basal planes with a definite diameter [5,6]. Carbon nanotubes are now considered as one of the most promising gas separation system.

However, to study the adsorption behavior via experiments is difficult because the microscopic properties of porous solids are often hard to determine. The techniques of molecular simulation are ideally suited to this study since model micropores and adsorbents can be defined in an unambiguous fashion on the computer. Gelb et al. [7] used Monte Carlo simulations in the semi-grand ensemble to study the wetting behavior and phase separation of a simple binary liquid mixture confined in a cylindrical pore. They regard the pore system as one-dimensional system. Although this system cannot exhibit true phase transitions, it showed a variety of phase separation behavior. They also studied the effect that increasing the degree of preferential adsorption of one species has on the “phase diagram” in these systems and found that dramatic shifts in the shape and position of the coexistence region can occur. Cracknell et al. [8] presented results for selective adsorption of a two-center Lennard–Jones model of ethane and a three-center Lennard–Jones model of propane in carbon slit pores, where they show the molecular shape and pore size play an important role in determining the extent of adsorptive separation. Besides, many other work have been carried out in the study of physisorbed mixtures, including molecular dynamics method [9,10], Monte Carlo method [11–14], and density functional theory [15].

In this work, grand canonical Monte Carlo (GCMC) method is used to study the adsorptive separation of the main products of water gas reaction, hydrogen and carbon monoxide. Single-walled carbon nanotubes are selected to be the adsorbent. We made a thorough and elaborate study on the effects of the packing geometry of carbon nanotubes on gas separation. To make a more comprehensive work, the influence of temperature as well as pressure on the separation is also studied. The simulation results in this work can be used to optimize the pore geometry for gas separation at a given pressure and temperature.

2. Potential models

In this work, all of the particles include hydrogen molecules, carbon monoxide molecules and carbon atoms are treated as structureless spheres. Particle–particle interactions between them are modeled with Lennard–Jones potential located at the mass-center of the particles. For a pair of particles i and j separated by the distance r , the interaction between them is given by

$$\phi_{ij}(r) = 4\varepsilon_{ij} \left[\left(\frac{\sigma_{ij}}{r} \right)^{12} - \left(\frac{\sigma_{ij}}{r} \right)^6 \right] \quad (1)$$

where i and j donate hydrogen, or carbon monoxide, or carbon particles, ε/k and σ are the energy and size potential parameters, which are 36.7 K and 0.296 nm for hydrogen, 100.2 K and 0.3763 nm for carbon

monoxide, and 28.2 K and 0.335 nm for carbon, respectively. Lorentz–Berthelot rules are used to calculate the parameters of interaction between different kinds of particles.

The general potential between a gas molecule and the nanotube is calculated by summing up pair interactions between individual carbon atoms and the gas molecules:

$$V(r) = \sum_j \phi_{ij}(|r_i - r_j|) \quad (2)$$

where r_i is the position of hydrogen or carbon monoxide molecule, r_j is that of a carbon atom and $\phi_{ij}(r)$ is the pair potential between a certain gas molecule and a carbon atom, while the sum is over all of the atoms on the tube.

Assuming that the atoms of the solid are distributed continuously up and on a sequence of parallel surfaces that form the pore wall, the interaction potential of the fluid molecule with one of these surfaces of area A and number density θ is given by [16]

$$V(r) = \int_A \theta v(r) d\alpha = 4\varepsilon_{\text{FC}}\theta \int_A \left[\left(\frac{\sigma_{\text{FC}}}{r} \right)^{12} - \left(\frac{\sigma_{\text{FC}}}{r} \right)^6 \right] d\alpha \quad (3)$$

where $\theta = 38 \text{ nm}^{-2}$, ε_{FC} and σ_{FC} are Lennard–Jones parameters of the interaction between fluid molecule and carbon atom. The fluids include hydrogen and carbon monoxide.

Integrating over the whole nanotube, the following expression can be obtained: [16]

$$V(r, R) = 3\pi\theta\varepsilon_{\text{FC}}\sigma_{\text{FC}}^2 \left[\frac{21}{32} \left(\frac{\sigma_{\text{FC}}}{R} \right)^{10} M_{11}(x) - \left(\frac{\sigma_{\text{FC}}}{R} \right)^4 M_5(x) \right] \quad (4)$$

where r is the distance between the adatom and the nearest point on the cylinder, R the radius of the nanotube, $x = r/R$ the ratio of distance to radius and θ the same surface number density as above. Here the following integrals are used:

$$M_n(x) = \int_0^\pi \frac{1}{(1 + x^2 - 2x \cos \varphi)^{n/2}} d\varphi \quad (5)$$

Simpson integration is used to get the final potential and some of the results are plotted in Fig. 1. Fig. 1a shows the situation of the tube with radius of 0.587 nm. Fig. 1b is that of the tube with radius of 0.9785 nm. In the figure, the interaction between carbon monoxide and the tube is stronger than that of hydrogen. Especially, the interaction of carbon monoxide is three times stronger inside the tube than that of hydrogen. However, as the tube becomes larger, the difference between these two fluids becomes smaller.

For simplicity of programming, the following expression was adopted to represent the results of the integration

$$\frac{V(r, R)}{\varepsilon} = a \left(\frac{\sigma}{R^{10}} \right) + b \left(\frac{\sigma^4}{R^4} \right) + c \left(\frac{\sigma^4}{R^3} \right) + d \left(\frac{\sigma^4}{R^2} \right) + e \left(\frac{\sigma^4}{R} \right) \quad (6)$$

where a – e are constants dependent on the kind of fluid and the R radius of the nanotubes. They can be determined from the numerical integration.

To binary system, the selectivity is defined as

$$S = \frac{x_1/y_1}{x_2/y_2} = \frac{\rho_{p2}^* \rho_{b1}^*}{\rho_{p1}^* \rho_{b2}^*} \quad (7)$$

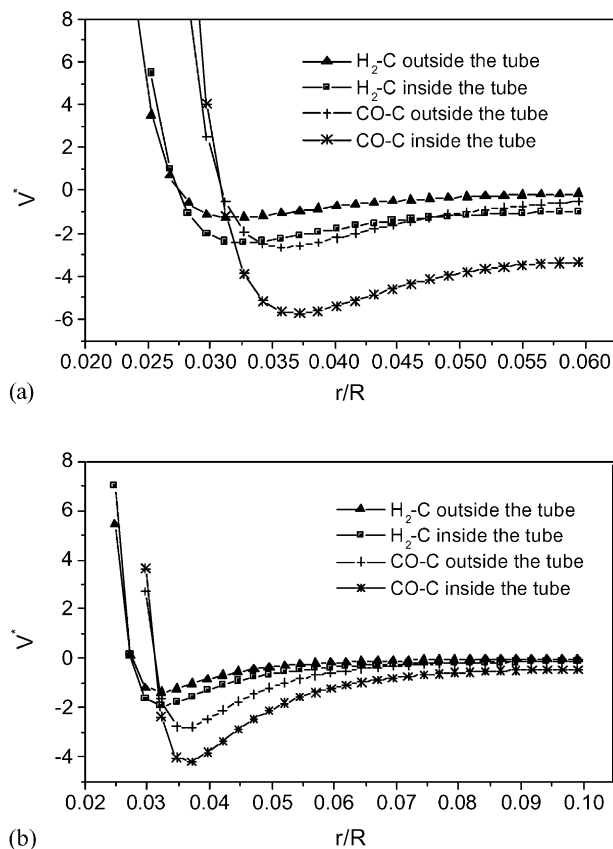


Fig. 1. The reduced potential ($V^* = V/\epsilon$) as a function of the distance between the hydrogen molecule and the nearest point on the cylinder: (a) $R = 0.587$ nm and (b) $R = 0.9785$ nm.

where x refers to a pore mole fraction and y to a bulk mole fraction. The subscripts of x and y refers to different components in the mixture. ρ_b^* is the reduced number density of the bulk fluid. ρ_p^* is that of the pore fluid.

3. Simulation method

First, Widom test particle method [17] in NVT ensemble is used to determine the relation between chemical potentials and the bulk pressures of the two components. The simulation is started with face centered cubic (fcc) structure, which involves 500 molecules. There are 250 molecules for hydrogen and carbon monoxide, respectively. One million configurations are used to reach equilibrium and another one million configurations are summed up to get the system average. Three test molecules of hydrogen or carbon monoxide are inserted into the system in each configuration to calculate the system potential. Systems with 11 different pressures are obtained in the simulation.

GCMC [17,18] is used in computing the adsorptive separation inside and outside single-walled carbon nanotubes (SWNTs). Five hundred molecules are placed as FCC structure to start the simulation. There

are 250 molecules for each component, respectively. Adsorbent materials are formed by an array of nanotubes arranged uniformly inside a cubic simulation cell. The axes of the nanotubes are parallel to the y direction. Periodic boundary conditions are employed in all three directions.

Three types of moves are involved in the GCMC method: (i) displacement; (ii) creation and (iii) deletion. The probabilities of making a displacement, a creation, and a deletion are equal. Spherical cut-off is used in the simulation. The cut-off distances are set to five times of Lennard–Jones size parameters of interactive particles, where Lorentz–Berthelot rules are used to determine the parameter between different species. Beyond this distance, Long-range corrections [18] are used to compensate the cut-off error. Four and a half million configurations are used to reach equilibrium and another 4.5 million configurations are summed up to get the ensemble average.

4. Results and discussions

Through Widom test particle method, the relation between the chemical potentials and system pressures of the two components can be obtained. The result is shown in Fig. 2. Generally speaking, the two chemical potential lines are alike. They increase with the pressures. When the pressures approach to zero, they approach to negative infinite. However, for higher pressure, the increase of the chemical potentials becomes slower and slower. The whole trend coincides with the definition of chemical potential exactly. Through the curve in Fig. 2, the analytic expression of chemical potentials can be obtained, which are

$$\mu_{\text{CO}}^* = -32.46 + 2.8604 \ln P^* \quad (8)$$

$$\mu_{\text{H}_2}^* = -56.317 + 7.95 \ln P^* \quad (9)$$

where Eq. (8) is the reduced chemical potential of carbon monoxide as a function of the reduced bulk pressure, Eq. (9) is that of hydrogen. Chemical potential and pressure are reduced by the Lennard–Jones potential parameters of hydrogen $\mu^* = (\mu/\varepsilon_{\text{H}_2})P^* = P \times (\sigma_{\text{H}_2}^3/\varepsilon_{\text{H}_2})$.

One of the configurations on x – z plane is shown in Fig. 3. The x – z plane is perpendicular to the axis of carbon nanotubes. Circles denote locations of carbon nanotubes. Small spheres are those of hydrogen molecules. Big ones are carbon monoxide molecules. It is clear that although in the bulk phase, the mole

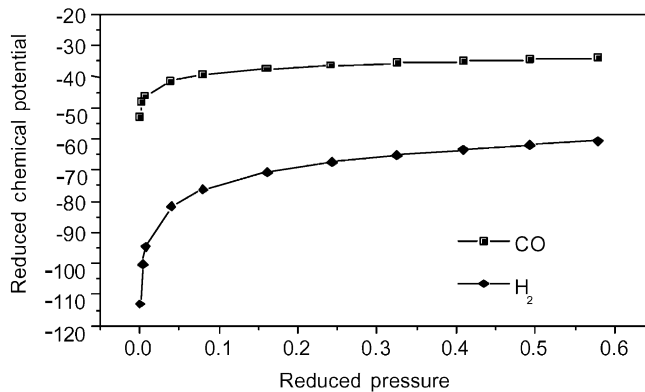


Fig. 2. The reduced chemical potential of H₂ and CO as function of reduced pressure at 293.15 K, $y_{\text{H}_2} = 0.5$.

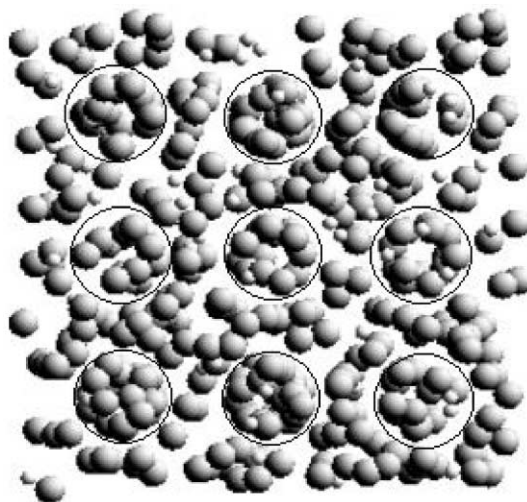


Fig. 3. One of the configurations at 293.15 K, 0.16 MPa. Big spheres denote CO molecules. Small ones denote hydrogen molecules. Circles are locations of carbon nanotubes. The radius of the tube is 0.9785 nm.

fraction of hydrogen is 0.5, the number of hydrogen molecules is far less than that of carbon monoxide in the pore phase. Thus, good separation effect of carbon nanotubes is manifest.

The gas mixture studied in this work consists of hydrogen and carbon monoxide. The two components have equal mole fraction 0.5 in the bulk phase. At 293.15 K, we have calculated the adsorption isotherms of both components in arrays of nanotubes with radius of 0.587 and 0.9785 nm, in which the van der Waals (VDW) distances (i.e. the distance between the walls of the nearest neighbor tubes in the bundle [19]) between tubes are fixed to 1 nm. The selectivity of the sorbent as a function of pressure was calculated as well. In both Fig. 4a and b, to given size of the nanotube, the adsorption of each component increases with pressure. At the same time, to each given pressure, the pore stores more carbon monoxide molecules than hydrogen. This is due to the stronger interaction between carbon monoxide and the tube wall. In Fig. 4a, the adsorption of carbon monoxide in the smaller tube ($R = 0.587$ nm) is almost twice than that in the bigger tube ($R = 0.9785$ nm). However, the adsorption of hydrogen in the smaller tube is far less than that in the bigger one. The two contrary results come from the coexistence of both components, which differs from the adsorption isotherm of any single one. There is a reasonable assumption that at given temperature, pressure and size of the tube, the total amount of gas in pore phase is close to a relatively fixed value. If it stores more of one component, the other will become less. When the smaller tubes are filled with the bigger carbon monoxide molecules, they have little spare space to store the small hydrogen molecules. On the contrary, the bigger tubes are more apt to stack more smaller hydrogen molecules. In Fig. 4c, the adsorptive selectivity decreases with the increase of pressure. This is because at higher pressures, packing effect becomes predominant in the adsorption. Therefore, the smaller hydrogen molecules are more apt to be packed in the tubes.

Fig. 5 shows the selectivity of carbon monoxide as a function of VDW distance. In both Fig. 5a and b, the selectivity inside the tube is higher than that outside the tube, especially in the smaller tubes (Fig. 5a). The reason can be traced back to Fig. 1, where the potential of carbon monoxide inside the tube is much bigger than that of hydrogen. Comparatively speaking, the discrepancy outside the

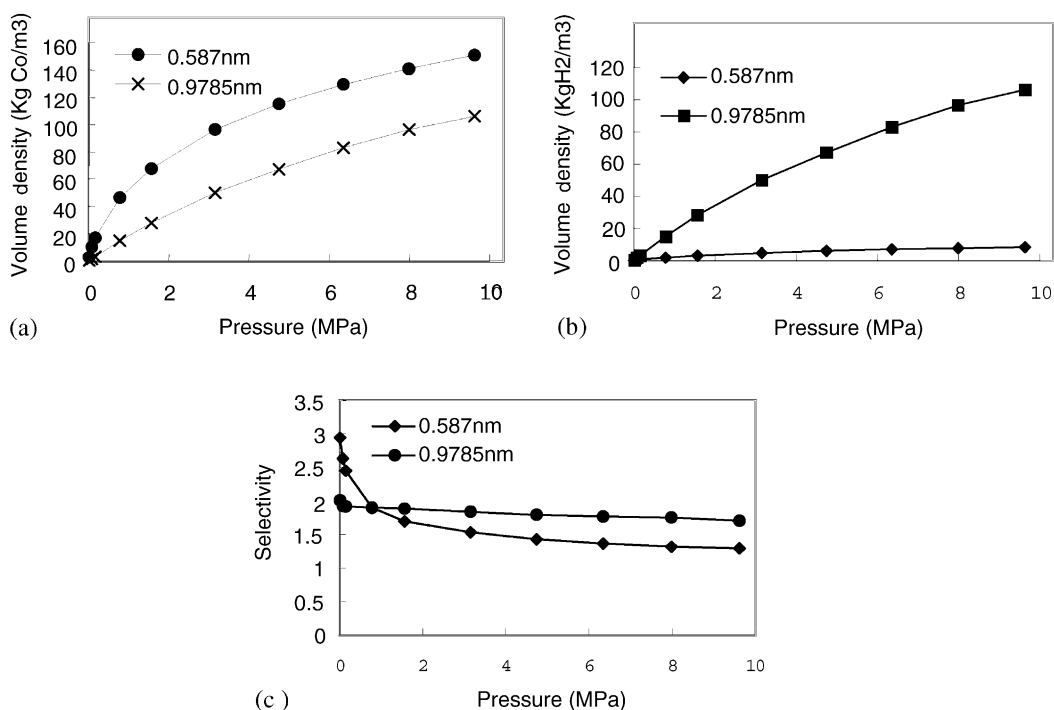


Fig. 4. (a) The adsorption isotherms of CO in nanotubes with radii of 0.587 and 0.9785 nm, (b) the adsorption isotherms of H₂ in nanotubes with radii of 0.587 and 0.9785 nm and (c) the selectivity of CO in nanotubes with radii of 0.587 and 0.9785 nm.

tube is not that much. Therefore, more carbon monoxide molecules are apt to be adsorbed inside the tube. As a result, the selectivity inside the tube is higher. However, along with the increase of tube size, the interactive potential of the two components come closer to each other. So it can be perceived that the discrepancy of selectivity inside and outside the tube becomes smaller with the increase of tube size.

In these two figures, the fluctuation of the selectivity along with the VDW distance is more violent in bigger tubes than that in smaller ones. There are three maximums in the former one, but only two in the latter. There are many factors that affect the amount of adsorption, two most important of which are the space and the attractive force [20]. The co-effect of these two factors forms the fluctuation of the adsorption of single component along with VDW distance. Moreover, these fluctuations often occur at the location of a new adsorptive layer. To gas mixtures, the situation becomes more complex. Generally speaking, more layers of particles can be stored in bigger tubes than in smaller ones. Therefore, there are more fluctuations along with VDW distance in bigger tubes than in smaller ones. However, as the VDW distance continues to increase, the attractive force reduces too much, which overwhelms the increase of space, so peaks of selectivity cease to emerge.

Fig. 6 shows the selectivity as function of nanotube radius at 293.15 K and 0.16 MPa. Here, we made an assumption that the radius of the nanotube can vary continuously. In the present study, under the pre-condition of the continuously and uniformly distributed carbon atoms on the cylinder, this assumption is quite a reasonable one. In these three figures, the selectivity fluctuates more rapidly than those

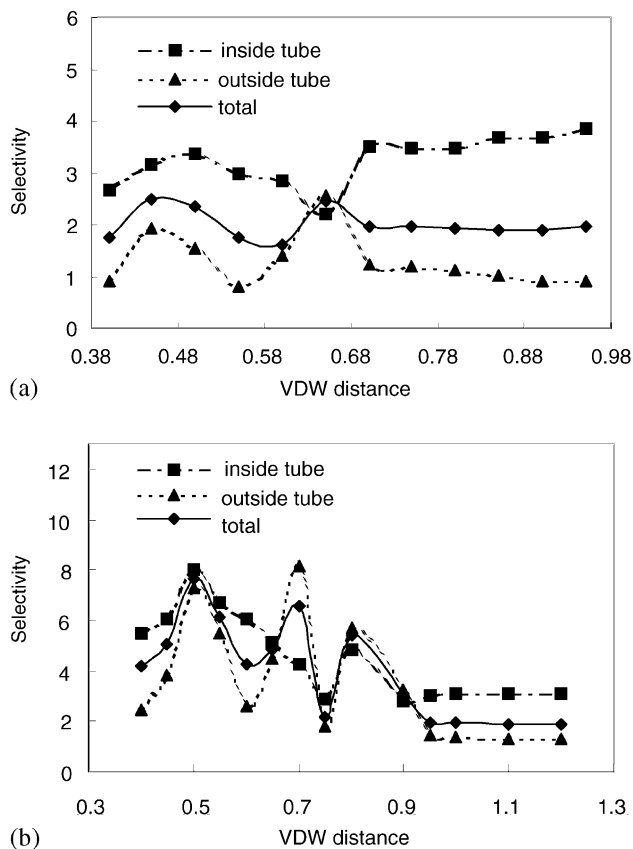


Fig. 5. The selectivity as function of VDW distance between tubes: (a) $R = 0.587$ nm and (b) $R = 0.9785$ nm.

in Fig. 5. In Fig. 6a and b, it can be concluded that, the fluctuation outside the tube is milder than that inside the tube. When the radius is relatively small (e.g. smaller than 0.5 nm), the increase of radius has little influence on selectivity outside the tube, whereas the selectivity inside the tube may reach a maximum almost 20 times of the minimum. However, when R is near 0.58 nm, the selectivity becomes very sensitive to the change of tube size. In some detail studies, it is found that even increase in radius by 10^{-5} nm, the selectivity can transfer from above 1 to below 1, i.e. in this circumstance, more hydrogen can be adsorbed than carbon monoxide. It is still not clear about the cause of this phenomenon.

The selectivity as a function of temperature is shown in Fig. 7, where the pressure is fixed at 0.1 MPa; the radius of the tube is 0.9785 nm and the VDW distance is 1 nm. In the figure, along with the increase of temperature, the selectivity increases rapidly to a maximum, then falls slightly down. This can be explained by the competition between two effects: the repulsive interaction between gas molecules and sorbents at short distances, and the strong attractive interaction between these molecules and sorbents at long distances. Attractive force is advantageous to the adsorption, but repulsive force not. For every temperature, there is a Mean field path (MFP) for each component. When the temperature is low, the MFP is short, which is in the range of repulsive interaction. Concluded from Fig. 1,

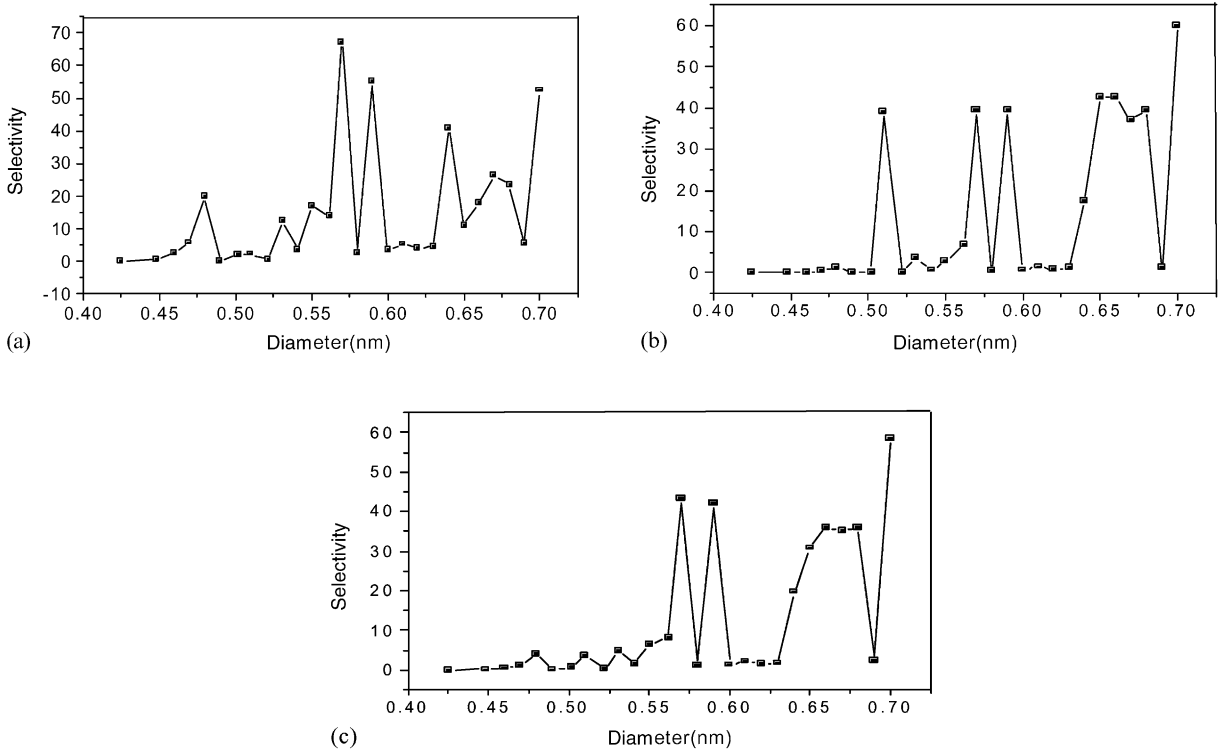


Fig. 6. The selectivity as function of carbon radius: (a) the selectivity inside the tube; (b) the selectivity outside the tube and (c) the total selectivity.

the repulsive force between carbon monoxide molecules and the sorbents decreases faster than that of hydrogen. Therefore, the adsorption of carbon monoxide increases faster, so that the selectivity increases at low temperature. On the other hand, at higher temperatures, the MFP is long, which is in the range of attractive interaction. In this circumstance, the attractive force between carbon monoxide molecules and the sorbents also decreases faster than that of hydrogen, which causes the adsorption of carbon monoxide decreases more rapidly than that of hydrogen. As a result, the selectivity falls down.

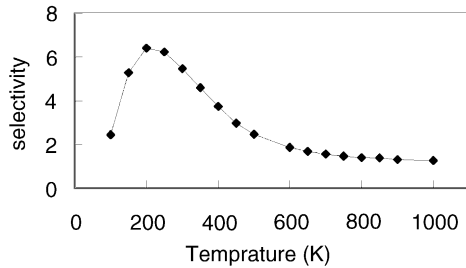


Fig. 7. The selectivity as a function of temperature.

5. Conclusions

In this paper, GCMC simulation is used to study the effect of temperatures, pressures and different structures of carbon nanotubes on the selectivity between hydrogen and carbon monoxide. The following conclusions can be obtained. The most basic one is, in most of the situations that the carbon nanotubes can adsorb more carbon monoxide than hydrogen. Then, at a given temperature and sorbent structure, the adsorption of hydrogen and carbon monoxide both increases with pressure. However, at higher pressures, the smaller hydrogen molecules are more apt to be packed in the pores, so that the selectivity of carbon monoxide decreases with the increase of pressure. Hence, increasing pressure is not advantageous to the separation of these two gases. However, under the co-effect of potential and space, there are several maximums of selectivity along with the increase of VDW distance. There are more and higher maximums in bigger pores and smaller VDW distances. Thus, a better separation can be obtained with bigger pore sizes and relatively small VDW distances. The selectivity along with the increase of tube radius fluctuates rapidly. Especially, there are some critical situations, where the selectivity becomes very sensitive to the change of radius. Therefore, an excellent separation effect can be probably obtained when varying the radius of the tube. Under the effects of repulsive interaction at short distances and attractive interaction at long distances, the selectivity has a peak along with the increase of temperature. As a result, choosing a proper temperature can greatly improve the separation. It is obvious through the above study that pressures, temperatures and sorbent structures are all important factors for the separation of gas mixtures. At last, we have to stress that our simulation results depend on our choice of intermolecular potentials, but such potentials seems to be a reasonable estimate of the interactions. More accurate models are being studied in the future.

Acknowledgements

We acknowledge the National Science and Technology Department through Hydrogen Energy Grant, no. 2000026400 and Tsinghua University Fundamental Study Fund.

References

- [1] J.H. Park, et al., Adsorber dynamics and optimal design of layered beds for multicomponent gas adsorption, *Chem. Eng. Sci.* 53 (23) (1998) 3951–3963.
- [2] S.U. Rege, et al., Sorbents for air pre-purification in air separation, *Chem. Eng. Sci.* 55 (2000) 4827–4838.
- [3] C.R. Clarkson, Binary gas adsorption/desorption isotherms: effect of moisture and coal composition upon carbon dioxide selectivity over methane, *Int. J. Coal Geol.* 42 (2000) 241–271.
- [4] S. Iijima, Helical microtubules of graphitic carbon, *Nature (London)* 354 (1991) 56–58.
- [5] E. Dujardin, et al., Capillarity and wetting of carbon nanotubes, *Science* 265 (5180) (1994) 1850–1852.
- [6] P.M. Ajayan, et al., Aligned carbon nanotube arrays formed by cutting a polymer resin–nanotube composite, *Science* 265 (1994) 1212–1214.
- [7] L.D. Gelb, K.E. Gubbins, Studies of binary liquid mixtures in cylindrical pores: phase separation, wetting and finite-size effects from Monte Carlo simulations, *Physica A* 244 (1997) 112–123.
- [8] R.F. Cracknell, et al., A grand canonical Monte Carlo study of Lennard–Jones mixtures in slit pores. 2. Mixtures of two-center ethane with methane, *Mol. Simulat.* 13 (3) (1994) 161–175.
- [9] I.M.J.J. Van de Ven-Lucassen, et al., Molecular dynamics simulation of the Maxwell–Stefan diffusion coefficients in Lennard–Jones liquid mixtures, *Mol. Simulat.* 23 (1) (1999) 43–54.

- [10] I.M.J.J. Van de Ven-Lucassen, et al., Molecular dynamics simulation of self-diffusion and Maxwell–Stefan diffusion coefficients in liquid mixtures of methanol and water, *Mol. Simulat.* 23 (1) (1999) 79–94.
- [11] V.Y. Gusev, J.A. O’Brien, Prediction of gas mixture adsorption on activated carbon using molecular simulations, *Langmuir* 14 (21) (1998) 6328–6331.
- [12] S. Samios, et al., Determination of micropore size distribution from grand canonical Monte Carlo simulations and experimental CO₂ isotherm data, *Langmuir* 13 (10) (1997) 2795–2802.
- [13] R.F. Cracknell, D. Nicholson, Adsorption of gas mixtures on solid surfaces, theory and computer simulation, *Adsorption* 1 (1) (1995) 7–16.
- [14] T.J.H. Vlugt, et al., Molecular simulations of adsorption isotherms for linear and branched alkanes and their mixtures in silicalite, *J. Phys. Chem. B* 103 (7) (1999) 1102–1118.
- [15] S.K. Bhatia, Adsorption of binary hydrocarbon mixtures in carbon slit pores: a density functional theory study, *Langmuir* 14 (21) (1998) 6231–6240.
- [16] G. Stan, M.W. Cole, Low coverage adsorption in cylindrical pores, *Surf. Sci.* 395 (1998) 280–291.
- [17] D. Frenkel, B. Smit, *Understanding Molecular Simulation*, Academic Press, New York, 1996. pp. 157–167.
- [18] M.P. Allen, D.J. Tildesley, *Computer Simulation of Liquids*, Clarendon Press, Oxford, 1987, pp. 126–131.
- [19] Q.Y. Wang, J.K. Johnson, Molecular simulation of hydrogen adsorption in single-walled carbon nanotubes and idealized carbon slit pores, *J. Chem. Phys.* 110 (1999) 577–586.
- [20] C. Gu, et al., Simulation study of hydrogen storage in single-walled carbon Nanotubes, *Int. J. Hydrogen Energy* 26 (2001) 691–696.